

AperTO - Archivio Istituzionale Open Access dell'Università di Torino

**The calculation of the static first and second susceptibilities of crystalline urea: A comparison of Hartree-Fock and density functional theory results obtained with the periodic coupled perturbed Hartree-Fock/Kohn-Sham scheme**

**This is the author's manuscript**

*Original Citation:*

*Availability:*

This version is available <http://hdl.handle.net/2318/70932> since

*Published version:*

DOI:10.1063/1.3267861

*Terms of use:*

Open Access

Anyone can freely access the full text of works made available as "Open Access". Works made available under a Creative Commons license can be used according to the terms and conditions of said license. Use of all other works requires consent of the right holder (author or publisher) if not exempted from copyright protection by the applicable law.

(Article begins on next page)



## UNIVERSITÀ DEGLI STUDI DI TORINO

**This is an author version of the contribution published on:**

M. Ferrero, B. Civalleri, M. Rerat, R. Orlando, R. Dovesi  
The calculation of the static first and second susceptibilities of crystalline urea: A comparison of Hartree-Fock and density functional theory results obtained with the periodic coupled perturbed Hartree-Fock/Kohn-Sham scheme.

*Journal of Chemical Physics*, 131, 214704, 2009,  
<http://dx.doi.org/10.1063/1.3267861>.

**The definitive version is available at:**

<http://jcp.aip.org>

**The calculation of the static first- and second-susceptibilities of crystalline urea. A comparison of HF and DFT (LDA, GGA, hybrid) results obtained with the periodic CP-HF/KS scheme.**

Mauro Ferrero,<sup>1</sup> Bartolomeo Civalleri,<sup>1</sup> Michel  
Rérat,<sup>2</sup> Roberto Orlando,<sup>3</sup> and Roberto Dovesi<sup>1</sup>

<sup>1</sup> *Dipartimento di Chimica IFM, Università di Torino and NIS  
-Nanostructured Interfaces and Surfaces - Centre of Excellence,  
<http://www.nis.unito.it> Via P. Giuria 7, 10125 Torino, Italy*

<sup>2</sup> *Equipe de Chimie Physique, IPREM UMR5254,  
Université de Pau, 64000 Pau, France*

<sup>3</sup> *Dipartimento di Scienze e Tecnologie Avanzate,  
Università del Piemonte Orientale, Via Bellini 25/G, 15100 Alessandria, Italy*

## Abstract

The static polarizability  $\alpha$  and first hyperpolarizability  $\beta$  tensors of crystalline urea and the corresponding first- ( $\chi^{(1)}$ ) and second- ( $\chi^{(2)}$ ) susceptibilities are calculated and compared with the same quantities obtained for the molecule by using the same code (a development version of CRYSTAL), basis set and level of theory. In order to separate geometrical and solid state effects, two geometries are considered for the molecule in its planar conformation: (i) as cut out from the bulk structure and (ii) fully optimized. First, the effect of basis sets on computed properties is explored at the B3LYP level by employing basis sets of increasing complexity, from 6-31G(d,p) to 6-311G(2df,2pd) (Pople's family) and from DZP to QZVPPP (Thakkar/Ahlrichs/Dunning's family) on  $\alpha$  and  $\beta$  for both the molecule and the bulk. Then, five different levels of theory, namely SVWN (LDA), PBE (GGA), PBE0 and B3LYP (hybrid) and HF are compared in combination with a TZPP basis set.

Present results shows that hybrid methods, in particular B3LYP, are remarkably successful in predicting correctly both the first- and second-susceptibility of urea bulk when combined at least with a triple-zeta quality basis set containing a double set of polarization functions. It is also shown that diffuse functions that are needed for molecular calculations are less crucial for the crystalline structure, as expected. Indeed, B3LYP/TZPP computed  $\chi^{(1)}$  and  $\chi^{(2)}$  tensor components ( $\chi_{aa}^{(1)} = 1.107$ ,  $\chi_{cc}^{(1)} = 1.459$  and  $\chi^{(2)} = -0.93$  a.u.) are in very good agreement with experimental values. At variance with respect to previous periodic ab-initio calculations, but in agreement with recent supermolecular results, the negative sign of  $\chi^{(2)}$  is confirmed.

Overall, static linear and non-linear optical properties such as dielectric constants, refractive and birefringence indices and second-harmonic generation coefficient of crystalline urea are very well reproduced by present calculations.

Keywords: urea, CPHF, periodic calculations, ab-initio, gaussian basis sets

## I. INTRODUCTION

The Coupled Perturbed Hartree-Fock (CPHF) method has recently been implemented in a development version of the CRYSTAL program<sup>1</sup> to compute the polarizability and dielectric tensor of solid state systems<sup>2,3</sup>. The implementation is based on the CPHF equations proposed by Hurst and Dupuis<sup>4</sup> and adapted to the periodic boundary condition context with reference to a local basis set consisting of Gaussian-type atomic orbitals<sup>5,6</sup>. Recently, we have also implemented the CPHF calculation of the first and second hyperpolarizabilities<sup>7</sup> showing that the method is equally accurate and suitable for the treatment of 0-, 1-, 2- and 3-dimensional systems. Finally, a generalization from CPHF to CPKS (Coupled Perturbed Kohn-Sham) for the polarizability tensor has been presented<sup>8</sup>, that can be extended to the first hyperpolarizability  $\beta$  tensor through the  $2n + 1$  approach. This generalization includes local- (LDA), semilocal- (GGA) and global hybrid-type HF/DFT functionals. In particular, hybrid methods that include exact HF exchange appear very promising because they allow to partly recover the correct asymptotic limit of the exchange-correlation potential and to partly compensate the spurious self-interaction error.

Here, we investigate the accuracy of our CP-HF/KS scheme in the calculation of the static (hyper)polarizability of crystalline urea by exploring the effect of the basis set and of the adopted exchange-correlation functional (i.e. LDA, GGA and hybrid). Urea has been considered as a case study of the wide family of molecular crystals with application in nonlinear optics. Indeed, molecular organic crystals are among the most promising materials for linear and nonlinear optics. The theoretical ab initio investigation of their optical properties has been mostly based on molecular approaches<sup>9</sup>. Basically, they rely on molecular calculations in which the effect of the surrounding molecules in the crystal structure is mimicked with different strategies. A recent account on the proposed schemes has been published by Champagne and Bishop<sup>9</sup> and we refer to that paper for a detailed discussion. In summary, most of those approaches are based on the calculation of the molecular (hyper)polarizability and then either an additivity assumption is made to estimate the corresponding first- and second-susceptibility of the crystalline structure or a multiplicative factor is used to include crystal environment effects. Also a supermolecule approach can be adopted but it can be rather expensive and an appropriate cluster must be carefully selected. All of those approaches work properly for weakly interacting molecules, but they are inadequate to deal with hydro-

gen bonded molecular crystals where long-range dipolar interactions and polarization effects take place and dominate the crystal packing. In this respect, crystalline urea is considered as a benchmark molecular crystal. Indeed, many experimental and theoretical works<sup>10-18</sup> have been done to measure and predict both first- ( $\chi^{(1)}$ ) and second-susceptibility ( $\chi^{(2)}$ ). In particular, we refer here to the recent work by Champagne and co-workers<sup>18</sup>. They reported on the attempt of using a supermolecule approach on a very large cluster by combining semi-empirical calculations (i.e. TDHF/AM1) with DFT and coupled-cluster methods through a multiplicative scheme. The idea is to include electron correlation effects by means of a multiplicative factor as obtained from high-level ab initio results on the isolated molecule. However, the predicted susceptibilities, in particular the linear response, were still underestimated with respect to experimental data especially the linear response. The authors then concluded that their approach could be limited by its inherent inability to account for long-range cooperative effects of the crystalline structure. The present full ab initio periodic approach that allows one to include all environmental effects due to the crystal packing, is therefore the most appropriate for a correct prediction of linear and nonlinear properties in hydrogen bonded molecular crystals. To our knowledge, so far, only two other periodic calculations were reported for crystalline urea by Lin et al.<sup>15</sup> and Levine and Allan<sup>11</sup> at the LDA level of theory within a planewaves/pseudopotentials theoretical framework. However, results were much larger than the experimental data because of the well known deficiency of the LDA approximation in reproducing correctly the band gap of solids.

In this work we show that: (i) the present implementation of the CPHF and CPKS scheme for periodic systems can be successfully applied to molecular crystals; (ii) hybrid HF/DFT functionals, such as B3LYP, give the best performance in predicting the first- and second-order susceptibility of urea; (iii) as for molecular calculations, the adopted Gaussian-type basis set must be at least of triple-zeta quality and must include diffuse  $s$  and  $p$  functions and two sets of polarization functions.

A detailed comparison of periodic calculations with the results for urea molecule as both cut out from the crystal and relaxed in its planar conformation ( $C_{2v}$ ) is also presented.

## II. COMPUTATIONAL DETAILS

Calculations were carried out with the periodic ab initio CRYSTAL06 program<sup>1</sup>. Crystalline orbitals are represented as linear combinations of Bloch functions (BF), and are evaluated over a regular three-dimensional mesh in reciprocal space. Each BF is built from atom-centered atomic orbitals, which are contractions (linear combinations with constant coefficients) of Gaussian-type functions (GTF), each GTF being the product of a Gaussian times a real solid spherical harmonic.

### A. Hamiltonians and basis sets

Along with the Hartree-Fock method, four different DFT methods were considered: the simplest density functional method, LDA in its SVWN parametrization<sup>19,20</sup>; the PBE GGA functional<sup>21</sup>, and two hybrid methods, B3LYP<sup>22-24</sup> (probably the most widely used hybrid functional in molecular calculations) in its VWN5 formulation, and PBE0<sup>25</sup> (also known as PBE1PBE or PBEh). The basis set dependence of computed results was investigated at the B3LYP level of theory by using twelve molecular all-electron basis sets. A first set of six basis sets was taken from the Pople's family of basis sets<sup>26</sup>, namely: 6-31G(d,p), 6-311G(d,p), 6-311G(2d,p), 6-311G(2d,2p), 6-311G(2df,p), 6-311G(2df,2pd). The second one ranges from DZP through TZP to QZVP basis sets as proposed by Thakkar et al.<sup>27</sup> (DZP and QZVP) and by Ahlrichs and co-workers<sup>28</sup> (TZP). The latter basis sets were further enriched by adding one or two more sets of *d* and *f* polarization functions from cc-pVXZ (X=T,Q) Dunning's sets to define the TZPP, QZVPP and QZVPPP basis. The number of basis functions in the unit cell ranges then from 152 (6-31G(d,p)) to 568 (QZVPPP). The comparison among HF and DFT methods was carried out by adopting the TZPP basis set.

### B. Computational parameters

The level of accuracy in evaluating the Coulomb and exchange series is controlled by five thresholds, for which values of  $10^{-7}$ ,  $10^{-7}$ ,  $10^{-7}$ ,  $10^{-7}$ ,  $10^{-18}$  were used for the Coulomb and the exchange series<sup>1</sup>. For the QZVPPP basis sets, tolerances were increased to  $10^{-7}$ ,  $10^{-7}$ ,  $10^{-7}$ ,  $10^{-12}$ ,  $10^{-36}$  and a Lowdin purification scheme was adopted with a screening on

the eigenvalues of the overlap matrix of  $10^{-4}$ . The DFT exchange-correlation contribution is evaluated by numerical integration over the cell volume<sup>29</sup>. Radial and angular points of the atomic grid are generated through Gauss-Legendre and Lebedev quadrature schemes. A grid pruning was adopted, as discussed in ref. 29. In the present study a (75,974)p grid has been used that contains 75 radial points and a variable number of angular points, with a maximum of 974 on the Lebedev surface in the most accurate integration region. The condition for the SCF convergence was set to  $10^{-7}$  on the root-mean-square variation of the density matrix elements between two subsequent cycles. The shrinking factor of the reciprocal space net was set to 4, corresponding to 18 reciprocal space points of the irreducible Brillouin zone at which the Hamiltonian matrix was diagonalized. The total energies obtained with this mesh are fully converged.

### C. Geometry optimization

In the solid state, urea forms a non-centrosymmetric tetragonal crystal that belongs to the  $P42_1m$  space group with two molecules in the unit cell as shown in Figure 1. Starting from the experimental crystal structure<sup>30</sup> at 12K (i.e.  $a=5.565 \text{ \AA}$  and  $c=4.684 \text{ \AA}$ ), a relaxation of the atomic coordinates by means of analytical energy gradients<sup>31-33</sup> was carried out at fixed lattice constants for each method and basis set. Lattice parameters were fixed because of the well known deficiency of DFT methods in dealing with weakly-bound systems. In this respect, the use of extended basis sets, such as TZP or larger, leads to a large overestimation of the cell size<sup>34</sup>.

The geometry optimization of the atomic positions was performed by means of a quasi-Newton algorithm in which the quadratic step (BFGS Hessian updating scheme) is combined with a linear one (parabolic fit) as proposed by Schlegel<sup>35</sup>. Convergence was tested on the RMS and the absolute value of the largest component of the gradients and the estimated displacements. The threshold for the maximum force, the RMS force, the maximum atomic displacement, and the RMS atomic displacement on all atoms have been set to 0.00045, 0.00030, 0.00180 and 0.00120 a.u., respectively. The optimization was considered complete when the four conditions are simultaneously satisfied. The crystal symmetry was maintained during the whole optimization process.



## D. Dielectric properties

Concerning the CPHF/CPKS calculation, the convergence was checked on the stability of the diagonal elements of the polarizability: the process stops when these elements differ by less than  $10^{-4}$  in two subsequent cycles.

The computed unit cell polarizability tensor components (i.e.  $\alpha_{ij}$ ) were transformed in the macroscopic first-order susceptibility tensor by using the following relation:

$$\chi_{ij}^{(1)} = \frac{4\pi}{V} \alpha_{ij} \quad (1)$$

where  $V$  is the unit cell volume. Similarly, the second-order susceptibility is derived from the corresponding unit cell first-hyperpolarizability  $\beta_{ijk}$  as

$$\chi_{ijk}^{(2)} = \frac{2\pi}{V} \beta_{ijk} \quad (2)$$

The dielectric tensor is then obtained as  $\epsilon_{ij} = \chi_{ij}^{(1)} + \delta_{ij}$  (where  $\delta_{ij} = 1$  if  $i = j$  and 0 for  $i \neq j$ ) while the refractive indices were evaluated according to the usual expression

$$n_{ii} = \epsilon_{ii}^{1/2} \quad (3)$$

Crystalline urea lacks of the center of inversion and shows nonlinear optical effects. Furthermore, it is a uniaxial crystal for which the first-susceptibility tensor shows two unique components  $\chi_{aa}^{(1)}$  and  $\chi_{cc}^{(1)}$  where  $a$  and  $c$  refer to the crystallographic axes. It is then birefringent with different refractive indices along the two main crystallographic axes. Two birefringence parameters are generally used<sup>36</sup>: the so-called linear birefringence

$$\Delta n = n_a - n_c \quad (4)$$

and

$$\delta^{(1)} = \frac{n_c - n_a}{n_a} \quad (5)$$

where  $n_a$  corresponds to the refractive index along the  $a$ -axis (ordinary) and  $n_c$  to the one along the  $c$ -axis (extraordinary).

According to the crystal symmetry, the second-susceptibility tensor of solid urea has only one non-zero component  $\chi_{abc}^{(2)}$ . From  $\chi_{abc}^{(2)}$ , the nonlinear coefficient  $d_{14}$  can be directly obtained as  $d_{14} = 1/2\chi_{abc}^{(2)}$  and related to second-harmonic generation measurements<sup>37</sup>.

As in ref. 18, also for the molecule, we adopt a coordinate system based on the main crystallographic directions of crystalline urea ( $a = b, c$ ). For the crystal, in the present notation  $\alpha_{aa(bb)} = \alpha_{xx(yy)}$ ,  $\alpha_{cc} = \alpha_{zz}$  and  $\beta_{abc} = \beta_{xyz}$ . It must be taken into account that the crystallographic directions have different orientations with respect to the Cartesian frame of the molecule, that lies in the  $y$ - $z$  plane with the CO bond oriented along the  $z$ -axis. In particular, while the  $c$ -axis is correctly oriented along the  $z$ -axis,  $a$  and  $b$  are oriented at  $45^\circ$  with respect to  $x$  and  $y$ , respectively. Therefore, for the free molecule,  $\alpha_{aa}$  is derived from  $\alpha_{xx}$  and  $\alpha_{yy}$ , and  $\beta_{abc}$  from  $\beta_{xxz}$  and  $\beta_{yyz}$ , through a rotation of  $45^\circ$ .

### III. RESULTS AND DISCUSSION

#### A. Molecular polarizabilities

Before discussing bulk dielectric properties, let us first focus on urea molecule. In the crystalline structure, the molecule adopts a planar conformation with  $C_{2v}$  symmetry (Figure 1); in contrast, in the gas phase the most stable structure has a  $C_2$  symmetry with the amino group assuming a pyramidal conformation with an *anti* configuration. To make a consistent comparison between the polarizability of the molecule alone and in the solid, we refer here to the planar conformation. We also take into account relaxation effects by considering the polarizability of the fully optimized molecular geometry (i.e. with the  $C_{2v}$  symmetry constraint) and the geometry as in the bulk structure.

##### 1. Effect of the basis set on molecular polarizabilities

Table 1 gathers the B3LYP molecular polarizability computed with the different basis sets employed in the present work comparing the polarizability of the molecule alone and in the crystal.

It is well known that polarizabilities are very sensitive to the quality of the basis set. Specific basis sets have been devised to properly predict electric properties of molecules as proposed by Sadlej and co-workers (see for instance ref. 38 and reference therein). Usually, they are augmented with rather diffuse  $s$  and  $p$  functions, but also diffuse polarization functions (i.e.  $d$  and even  $f$  functions) are needed. In periodic system, the role of these basis

functions is less crucial. Because of the crystal packing, the molecule can take advantage from the atomic functions centered on neighboring molecules to improve the description of the wavefunction. This can be seen by comparing results for the free molecule obtained with basis sets containing very diffuse functions such as the aug-cc-pVTZ and the Sadlej-pVTZ basis sets that can be considered as a reference. The B3LYP computed values of  $\alpha_{aa}$  ( $\alpha_{cc}$ ) are 34.483 (41.744) a.u. and 34.766 (42.162) a.u. for the two basis sets, respectively. Results of Table 1 confirm the marked basis set dependence of the polarizability. In particular, the effect is larger for  $\alpha_{aa}$  than  $\alpha_{cc}$  (i.e. the out-of-plane polarizability  $\alpha_{xx}$  is more sensitive to the basis set quality). In the molecule, the role of the diffuse functions is clearly highlighted when the TZPP basis set is enriched with the same augmented basis functions as in the aug-cc-pVTZ basis. The computed data pass from 28.718 and 37.129 a.u. to 33.755 and 40.778 a.u., very close to the reference basis sets with a substantial improvement of  $\alpha_{aa}$ . However, when the molecular polarizabilities of the molecule in the crystal are considered, the dependence on the basis set is less critical. Indeed, TZPP, QZVPP and QZVPPP results are fairly close to each other. This shows that in the solid the molecular polarizability is less sensitive to the basis set when a good quality set of atomic functions is adopted.

Overall, computed values improve when: (i) passing from Pople’s to more flexible Ahlrichs/Thakkar basis sets; (ii) removing the *sp*-constraint (e.g. 6-311G(2df,2p) vs TZPP); (iii) including low exponents Gaussian functions both of *s,p*-type, as from DZP through TZP to QZVP (e.g. for carbon, the lowest exponent is less than 0.10 a.u.), and *d,f* polarization functions, as from TZP to TZPP or in the series QZVP, QZVPP and QZVPPP (e.g. for carbon, *d* and *f* lowest exponents are 0.23 and 0.49 a.u., respectively). It is worth noting that at least two sets of polarization functions (i.e.  $2d+f$  AOs) are necessary to obtain reasonable results.

From Table 1, we can also observe that:

- Polarizabilities of the free molecule in the relaxed geometry and as in the bulk differ slightly. A larger difference is observed for  $\alpha_{cc}$  in the unrelaxed structure because the effect of the crystalline environment is to elongate the CO bond that is involved in four hydrogen bonds: two along the infinite chains and two with the neighboring chains oriented in the opposite direction (see Figure 1). Strong dipole-dipole interactions are involved in the bonding along the chains thus contributing to give longer CO bonds.

- The effect of the intermolecular interactions is evident when considering the ratio between the polarizability of the molecule in the crystal and the free molecule (see Table 1). that ranges from 1.54 and 1.43 for  $\alpha_{aa}$  and from 1.57 to 1.46 for  $\alpha_{cc}$ . As expected, a more significant increase is observed along the  $c$ -axis, where the molecules are oriented head-to-tail to form infinite chains, (see Figure 1) as a consequence of dipole-dipole interactions, hydrogen bonding and charge transfer effects. Indeed, as reported by Whitten et al.<sup>17</sup>, the dipole moment of the molecule increases from 3.83 D in the gas phase to 6.56 D in the solid state, with the latter being estimated from synchrotron X-ray structure factors<sup>39</sup>. Also, the comparison of the Born charges (i.e. charges derived from first-derivative of the cell polarizability with respect to normal modes in the Cartesian frame<sup>40,41</sup>) of the molecule alone and in the crystal allows us to rationalize the enhancement of the molecular polarizabilities. For instance, for the carbonyl group, the Born charge on the oxygen atom increases from -0.85 to -1.50  $e$ , while carbon passes from 1.42 to 1.93  $e$ . A similar increment is also observed for nitrogen and hydrogen. This shows that a large redistribution of the charge density of the molecule takes place in the crystalline structure. The enhancement reduces when enriching the basis set: extended basis sets provide a better description of the polarizability of the isolated molecule with respect to the crystal where it has already converged.
- Although  $\alpha_{cc}$  and  $\alpha_{aa}$  for the free molecule and the one in the crystalline structure are very different to each other because of the crystalline environment, their ratio (i.e.  $\alpha_{cc}/\alpha_{aa}$ ) is rather similar in the two systems, being around 1.3-1.5; it tends to reduce when enriching the basis set. This is an evidence that larger basis sets allow a better description of the out-of-plane polarizability (i.e.  $\alpha_{aa}$ ). For instance, passing from DZP to QZVPPP there is a remarkable increase of  $\alpha_{aa}$  while for  $\alpha_{cc}$  this effect is less evident. In this respect, results show that basis set convergence is more rapid for  $\alpha_{cc}$  than  $\alpha_{aa}$  for both the molecule alone and in the crystal.

Overall, results indicate that in the trade-off between cost and accuracy, the TZPP basis set is rather satisfactory being in semi-quantitative agreement with the data computed with very large basis sets. Therefore, it has been used in the following section as a reference to compare HF and DFT results.

## 2. Effect of the level of theory

The molecular polarizabilities of urea both isolated and in the crystal calculated with different DFT methods and at HF level are given in Table 2. It is evident that electron correlation effects at the DFT level are quite relevant. For the free molecule they are of the order of 12% to 22% with the lower value corresponding to the hybrid functionals, while it increases for GGA and LDA functionals (i.e. PBE and SVWN). An increment of the polarizabilities of 15-20% agrees with previously reported MP2 and CCSD results obtained with larger basis sets by Reis et al.<sup>12</sup> and Olejniczak et al.<sup>18</sup>, respectively.

As already discussed, structural changes in the molecule due to the crystal packing lead to a slight increment of the polarizability. On the contrary, full inclusion of crystalline environment and electron correlation effects remarkably increases the polarizabilities of the molecule in the unit cell. In this case, electron correlation is very important giving a contribution of more than 20-25% for hybrid methods, 35-40% for GGA and 40-45% for LDA. The effect is more relevant for  $\alpha_{cc}$  than  $\alpha_{aa}$  because electron correlation makes electrostatic and charge transfer effects stronger along the  $c$ -axis. As expected, those effects are more marked at the LDA level because of the known tendency to delocalize the charge density. This reduces when passing to GGA and hybrid functionals, as clearly seen from Table 2.

Also given in Table 2 are the enhancement of the polarizabilities when the molecules are packed to form the crystal. Again, electron correlation plays a significant role. The enhancement is larger for LDA and GGA while decreases when adding some exact HF exchange. Although predicted polarizabilities of urea molecule in the crystal are slightly different for PBE0 and B3LYP, nevertheless the enhancement factors are the same.

Interestingly, as already pointed out in the previous section, the  $\alpha_{cc}/\alpha_{aa}$  ratio is roughly independently of the adopted level of theory being  $\sim 1.3$  for both the isolated molecule and the crystal .

## B. Bulk first-order susceptibilities

### 1. Basis set dependence

From the data of Table 1 for urea crystal the static first-order susceptibility and related dielectric properties can be computed by using equations 1 and 3. Table 3 reports the optical dielectric properties of urea crystal determined at the B3LYP level as a function of the basis set size in comparison with experimental values for the optical dielectric tensor components extrapolated to the static limit through a Sellmeier equation<sup>37</sup>. From experimental tensor components the refractive indices can be obtained as well as birefringence parameters to be compare with computed results.

The birefringence parameters can be analyzed as indicators of the anisotropy of the electric-response of the crystal to the perturbation. Small basis sets lead to an unbalanced description of the susceptibility favoring the  $cc$  component with respect to the  $aa$  one. The inclusion of more diffuse functions and two sets of polarization functions, as in the TZPP basis set, provide a significant improvement of  $\delta^{(1)}$  and  $\Delta n$  thus confirming that the basis set must be sufficiently flexible to allow the proper description of the wavefunction both in the plane and out of the plane of the molecule. In this respect, results obtained with the largest basis set, i.e. B3LYP/QZVPPP, are in excellent agreement with experimental values.

Figure 2 (a) shows the deviation of computed data from experiment as a function of the basis set whereas in Figure 2 (b) the dielectric tensor components are plotted as a function of the number of atomic orbitals in the unit cell. The two figures show that (i) the deviation from experiment remarkably reduces when enriching the basis set and (ii) a near-convergence to the complete basis set limit is reached. Hence, the QZVPPP basis set provides predictions that can be considered as benchmark values for the B3LYP functional. As expected from the previous discussion on the molecular polarizabilities, Pople’s basis sets reach limit values that are far from the experimental data, while TZ and QZ basis sets systematically improve approaching quite closely the experimental values, in particular when more and more polarization functions are included.

Two other aspects deserve further discussion:

- It must be pointed out that the refractive indices are calculated from the unit cell volume (see eq. 1) fixed at its experimental value at 12 K. However, observed refractive indices are usually measured at room temperature. The role of thermal expansion effects was then estimated at the B3LYP level by computing the unit cell polarizability with lattice parameters fixed at 123 K and 295 K as determined from X-ray diffraction experiments<sup>39</sup>. The corresponding refractive indices are:  $n_{aa}=1.449$ ,  $n_{cc}=1.566$  and  $n_{aa}=1.436$ ,  $n_{cc}=1.552$ , respectively. As expected, the computed values decrease when the volume increases. In comparison to results for the 12 K unit cell, the decrease of  $n$  is larger between 123 K and 295 K. This is due to the substantial increase of the cell volume in that range of temperature. Interestingly, the largest variation is observed for  $n_{aa}$  in agreement with experimental evidence that shows a larger thermal expansion for the  $a$ -axis<sup>42</sup>. Overall, the effect of the choice of the reference unit cell volume is small with a percentage variation no larger than 1%. Therefore, in the present work, all reported results refer to the unit cell volume at 12 K.
- From computed data, also the  $\omega = 0$  limit can be obtained by including the contribution from nuclear vibrational motion<sup>41</sup>. Using the vibrational frequencies at the  $\Gamma$  point<sup>29</sup> computed at the B3LYP/TZPP level, the static dielectric tensor components at the zero wavelength limit are  $\epsilon_{aa}^0=3.771$  and  $\epsilon_{cc}^0=2.972$  a.u.. It is worthy to note that: (i) the vibrational contribution is quite large; (ii) the calculation of the  $\omega = 0$  vibrational effect is based on a double harmonic approximation; (iii) it is appropriate to ignore vibration in comparing with extrapolated (to  $\omega = 0$ ) measurement because vibrations do not contribute in the high  $\omega$  limit where measurements are made.

## 2. *Effect of the level of theory*

In Table 4 the dielectric properties of crystalline urea computed with LDA, GGA and hybrids methods along with HF are reported. Results are also compared with other predicted theoretical data and experimental values. As expected from Table 2, computed results show the same trend as discussed for the molecular polarizabilities, with the SVWN (LDA) dielectric tensor components and refractive indices being larger than PBE (GGA), hybrids functionals and HF, in the order. LDA and GGA data are also overestimated with respect to experimental values<sup>37</sup> while hybrid methods are in rather good agreement, in particular the

B3LYP functional. On the contrary, HF gives definitely underestimated refractive indices highlighting then the crucial role played by electron correlation for a correct prediction of the dielectric properties of urea.

In the comparison between HF and DFT, an inverse correlation is clearly observed between the predicted dielectric tensor components and the computed band gap of crystalline urea. Reported band gap decreases in the series: HF > hybrids > GGA > LDA, while, on the opposite,  $\epsilon_{aa}$  and  $\epsilon_{cc}$  increase. This is not unexpected because polarizability is largely determined by the response of the electronic structure to the perturbation of the electric field and also depends on the correct asymptotic behaviour of the exchange-correlation potential ( $v_{xc}$ ). Also, the band gap is directly involved in the expression of the polarizability (see ref. 8 for details). Energy level differences appear at the denominator thus lowering the polarizability when increasing the energy gap. HF shows the right decay but predicts a too large band gap. Unlike LDA and GGA functionals, hybrid methods reduce the self-interaction error and partly recover the correct asymptotic behaviour of  $v_{xc}$ . This, combined with a better predicted band gap leads to a good agreement with experiment. In comparing B3LYP and PBE0, it seems that a lower amount of HF exact exchange as in B3LYP (i.e. 20%) gives better results than for PBE0 in which it amounts to 25%. However, the reduction of exact exchange would lead to a worsen long-range decay of  $v_{xc}$ . In this respect, newly developed range-separated hybrid methods<sup>43</sup> (i.e. long-range corrected hybrids) have been shown to be more accurate than global hybrid functionals<sup>44</sup>, as B3LYP and PBE0, and deserve to be considered in future works. On passing, we also point out that band gap is substantially independent of the basis set size. Also, it is worth noting that, as expected from discussion on basis set dependence, TZPP results are slightly underestimated and then larger basis sets should increase the already overestimated LDA and GGA results.

Electron correlation is important to give the right balance between ordinary and extraordinary refractive indices as expresses by  $\delta^{(1)}$  and  $\Delta n$ . At HF level, both are underestimated while increase for the DFT methods. In particular, hybrid methods are in very good agreement with experiment while LDA and GGA provide slightly overestimated results. This confirms that LDA and GGA methods give unbalance electron correlation effects that favor an increase of the crystal polarizability along the  $c$ -axis.

From Table 4, a comparison with other theoretical published data can be done. Present LDA results favorably compare with previously reported data, in particular, with the one



from ref. 15 obtained within a pseudopotentials/planewaves computational approach, although not computed at the static limit. Moreover, it can be seen that the supermolecule approach as adopted by Champagne and co-workers<sup>18</sup> is not satisfactory being largely underestimated, even if corrections were included to take into account electron correlation effects. Data calculated within the frame of the rigorous local-field theory both by Munn and co-workers<sup>12</sup> at the MP2 level and by Whitten et al.<sup>17</sup> from a X-ray fitted wavefunction are in good agreement with experiment. Even though, both overestimate the crystal polarizability along the  $c$ -axis showing a better agreement for  $\epsilon_{aa}$  than  $\epsilon_{cc}$ . It must be pointed out that the comparison with previous works could be partly biased by the different choices of the reference crystalline structure adopted for the calculation. Nevertheless, the comparison shows that data computed at the B3LYP level of theory with the present fully periodic approach are in excellent agreement with experiment.

### C. Molecular hyper-polarizability and bulk second-order susceptibility

In Table 5 are given the calculated molecular (first)hyper-polarizability and bulk second-order susceptibility. Reported results refer to both B3LYP calculations with different basis sets and HF and DFT predictions obtained with the TZPP basis set.

It is well known from molecular calculations that hyper-polarizability is even more sensitive than polarizability towards basis set quality and electron correlation effects (see for instance ref. 38). Apparently, from Table 5, B3LYP hyper-polarizabilities show a small basis set dependence for the molecule both alone and in the crystal. However, if for the free molecule larger basis sets are adopted, such as the aug-cc-pVTZ or the Sadlej-pVTZ,  $\beta_{abc}$  is -35.735 and -36.024 a.u., respectively, showing that the quality of the basis set is crucial. As discussed for the polarizability, the major role is played by diffuse  $s,p$  but also  $d,f$  atomic functions. When the TZPP is enriched with a set of diffuse  $s,p,d$  functions the value of  $\beta_{abc}$  becomes -32.714 a.u., very close to larger basis sets. Since  $\beta_{abc}$  is derived from  $\beta_{xxz}$  and  $\beta_{yyz}$ , it is worthy to note that again the major contribution of diffuse functions is for the out-of-plane component  $\beta_{xxz}$ . Although the difference with more extended basis sets seems quite large, we believe that such diffuse functions are useless for crystalline systems, as already pointed out before. Therefore, the adopted basis sets are considered a reasonable choice.

Electron correlation effects are remarkably large with an enhancement of  $\beta_{abc}$  due to the

crystal field even more significant than for the polarizability. The trend observed is the same, with LDA, GGA and hybrid methods being larger than HF, in the order. The inclusion of HF exact exchange in hybrid functional leads to results in between GGA and HF. In this case, the same arguments on the role of the band gap used for  $\alpha_{aa(cc)}$  also hold for  $\beta_{abc}$ . For the molecule, SVWN and PBE provide very low values for  $\beta_{abc}$  with respect to HF and hybrids. As already pointed out by Benková et al.<sup>45</sup> in comparison with high level CCSD(T) calculations, this is due to an overall underestimation of the  $\beta_{xxz}$  component at DFT level, but also  $\beta_{yyz}$  results to be problematic with LDA and GGA functionals. Moreover, with those methods, the charge density is more polarized along the molecular  $z$ -axis (i.e. along the C=O bond) than at HF level and with hybrids.

No experimental value for the second-order susceptibility are available at the static limit. Nevertheless, measurements of  $d_{14}$  at 597 and 1064 nm of  $1.3\pm 0.3$  and  $1.2\pm 0.1$  pm/V, respectively, indicate that the dispersion to the static limit is not significant given the substantial error bars and the large band gap of urea.<sup>11</sup> Therefore, this suggests that at the static limit a reasonable value for the second-order susceptibility of urea could be  $1.0\pm 0.2$  pm/V.

Hybrid methods give slightly underestimated results while GGA and LDA are close to the observed estimation. Indeed,  $d_{14}$  ranges from -0.86 to -1.15 pm/V for all of the DFT methods in substantial agreement with experiment and well within the experimental uncertainty, even if the estimated experimental error bar is rather large being  $\pm 20\%$ . This indicates that for qualitative purposes also LDA and GGA functionals can be used to predict linear and nonlinear optical properties of crystalline urea.

Furthermore, we point out that the sign of  $\chi_{abc}^{(2)}$  cannot be determined from experimental measurements. Hence, according to present crystallographic directions, results show that independently of the level of theory  $\chi_{abc}^{(2)}$  has a negative sign. This finding is in contrast with previous periodic ab-initio calculations<sup>15</sup>, but in agreement with respect to recent supermolecular results<sup>18</sup>.

Finally, it is worthy to note that the vibrational contribution to  $\chi_{abc}^{(2)}$  might very well have an even larger effect than it does on  $\chi_{aa(cc)}^{(1)}$  where it is already quite large. Although it is not yet possible, to our knowledge, to compute it for crystalline systems, in principle it could be estimated as the difference between measured second harmonic generation and Pockels effect.

## IV. CONCLUSIONS

The present work shows that the macroscopic optical susceptibilities of crystalline urea can be reliably predicted through a fully periodic CPHF/KS approach developed for HF and DFT methods and atom-centered basis functions as implemented in the CRYSTAL code. In particular, hybrid HF/DFT functionals, such as B3LYP, give good performance in predicting the first- and second-order susceptibility of urea.

We have carefully investigated the appropriate description of the wavefunction employing twelve basis sets of increasing size and quality at the B3LYP level of theory. The basis set must be of TZ quality and include Gaussian functions with low exponents (i.e. less than 0.1 a.u.), compatible with the periodic nature of the crystal, and also first- and second-order polarization functions (i.e.  $d$  and  $f$ ). In particular, at least two sets of polarization functions (i.e.  $2d, f$  on heavy atoms and  $2p, d$  on hydrogen) are needed, in agreement with evidence for molecules as demonstrated in the construction of the Sadlej’s basis sets especially devised to reproduce molecular (hyper)polarizability. As expected, dependence on the basis set quality is more delicate for hyper-polarizability ( $\beta$ ) than polarizability ( $\alpha$ ). However, because of the periodic nature of the crystalline wavefunction, basis set requirements are less critical than for molecules.

Electron correlation effects are very important for a correct description of the response of crystalline urea to electric fields through its role on intermolecular interactions. For DFT methods, the inclusion of exact exchange is shown to be substantial to reduce the effect of the self-interaction error on the electronic structure and partly recover the correct asymptotic limit of the exchange-correlation potential.

Overall, the present fully periodic CP-HF/KS scheme offers, at variance with other approaches, two important advantages. It allows (i) the consistent inclusion of crystal environment effects and (ii) the use of hybrid DFT methods. Hence, it offers an accurate computational tool to predict the linear and nonlinear optical properties of molecular crystals and, in perspective, it can be fruitfully applied for the development of new and improved molecular materials.

Work is in progress to extend present approach to third-order susceptibility,  $\chi^{(3)}$  and to include frequency dependence.

## V. ACKNOWLEDGEMENTS

Authors are grateful to Prof. B. Kirtman for reading the manuscript and for useful discussions and suggestions. RD acknowledges financial support from MIUR (Project COFIN2007, Prot. 200755ZKR3 004).

- <sup>1</sup> Crystal06 user's manual. Dovesi, R.; Saunders, V. R.; Roetti, C.; Orlando, R.; Zicovich-Wilson, C. M.; Pascale, F.; Civalleri, B.; Doll, K.; Harrison, N. M.; Bush, I. J.; D'Arco, P. and Llunell, M.; Università di Torino, Torino, 2006.
- <sup>2</sup> Ferrero, M.; Rérat, M.; Orlando, R. and Dovesi, R., *Computation in Modern Science and Engineering*, Vol. 2B, T. E. Simos and G. Maroulis, American Institute of Physics, 2007.
- <sup>3</sup> Ferrero, M.; Rérat, M.; Orlando, R. and Dovesi, R., *J. Comp. Chem.*, 2008, **29**, 1450.
- <sup>4</sup> Hurst, G. J. B. and Dupuis, M., *J. Chem. Phys.*, 1988, **89**, 385.
- <sup>5</sup> Kirtman, B.; Gu, F. L. and Bishop, D. M., *J. Chem. Phys.*, 2000, **113**, 1294.
- <sup>6</sup> Kudin, K. N. and Scuseria, G., *J. Chem. Phys.*, 2000, **113**, 7779.
- <sup>7</sup> Ferrero, M.; Rérat, M.; Kirtman, B. and Dovesi, R., *J. Chem. Phys.*, 2008, **129**, 244110.
- <sup>8</sup> Ferrero, M.; Rérat, M.; Orlando, R.; Dovesi, R. and Bush, I., *J. Phys. Conf. Series*, 2008, **117**, 012026.
- <sup>9</sup> Champagne, B. and Bishop, D. M., *Adv. Chem. Phys.*, 2003, **126**, 41.
- <sup>10</sup> Perez, J. and Dupuis, M., *J. Chem. Phys.*, 1991, **95**, 6525.
- <sup>11</sup> Levine, Z. H. and Allan, D. C., *Phys. Rev. B*, 1993, **48**, 7783.
- <sup>12</sup> Reis, H.; Papadopoulos, M. G. and Munn, R. W., *J. Chem. Phys.*, 1998, **109**, 6828.
- <sup>13</sup> Reis, H.; Papadopoulos, M. G.; Hättig, C.; Ángyán, J. G. and Munn, R. W., *J. Chem. Phys.*, 2000, **112**, 6161.
- <sup>14</sup> Wu, K.; Snijders, J. G. and Lin, C., *J. Phys. Chem. B*, 2002, **106**, 8954.
- <sup>15</sup> Lin, Z.; Wang, Z.; Chen, C. and Lee, M.-H., *J. Chem. Phys.*, 2003, **118**, 2349.
- <sup>16</sup> Skwara, B.; Gora, R. W. and Bartkowiak, W., *Chem. Phys. Lett.*, 2005, **406**, 29.
- <sup>17</sup> Whitten, A. E.; Jayatilaka, D. and Spackman, M. A., *J. Chem. Phys.*, 2006, **125**, 174505.
- <sup>18</sup> Olejniczak, M.; Pecul, M.; Champagne, B. and Botek, E., *J. Chem. Phys.*, 2008, **128**, 244713.
- <sup>19</sup> Dirac, P. A. M., *Proc. Cambridge Philos. Soc.*, 1930, **26**, 376.

- <sup>20</sup> Vosko, S. H.; Wilk, L. and Nusair, M., *Can. J. Phys.*, 1980, **58**, 1200.
- <sup>21</sup> Perdew, J. P.; Burke, K. and Ernzerhof, M., *Phys. Rev. Lett.*, 1996, **77**, 3865.
- <sup>22</sup> Becke, A. D., *J. Chem. Phys.*, 1993, **98**, 5648.
- <sup>23</sup> Lee, C.; Yang, W. and Parr, R. G., *Phys. Rev. B*, 1988, **37**, 785.
- <sup>24</sup> Miehlich, B.; Savin, A.; Stoll, H. and Preuss, H., *Chem. Phys. Lett.*, 1989, **157**, 200.
- <sup>25</sup> Adamo, C. and Barone, V., *J. Chem. Phys.*, 1999, **110**, 6158–6170.
- <sup>26</sup> Hehre, W. J.; Radom, L.; v. R. Schleyer, P. and Pople, J. A., *Ab Initio Molecular Orbital Theory*, Wiley, New York, 1986.
- <sup>27</sup> Thakkar, A. J.; Kogan, T.; Saito, M. and Hoffmeyer, R. E., *Int. J. Quantum Chem.*, 1993, **27**, 343.
- <sup>28</sup> Schäfer, A.; Horn, H. and Ahlrichs, R., *J. Chem. Phys.*, 1992, **97**, 2571.
- <sup>29</sup> Pascale, F.; Zicovich-Wilson, C. M.; Gejo, F. L.; Civalleri, B.; Orlando, R. and Dovesi, R., *J. Comp. Chem.*, 2004, **25**, 888.
- <sup>30</sup> Swaminathan, S.; Craven, B. N. and McMullan, R. K., *Acta Crystallogr. Sec. B*, 1984, **40**, 300.
- <sup>31</sup> Doll, K.; Saunders, V. R. and Harrison, N. M., *Int. J. Quantum Chem.*, 2001, **82**, 1–13.
- <sup>32</sup> Doll, K., *Computer Physics Communications*, 2001, **137**, 74–88.
- <sup>33</sup> Doll, K.; Dovesi, R. and Orlando, R., *Theor. Chem. Acc.*, 2004, **112**, 394.
- <sup>34</sup> Civalleri, B.; Doll, K. and Zicovich-Wilson, C. M., *J. Phys. Chem. B*, 2007, **111**, 26.
- <sup>35</sup> Schlegel, H. B., *J. Comp. Chem.*, 1982, **3**, 214.
- <sup>36</sup> Rosker, M. J.; Cheng, K. and Tang, C. L., *IEEE J. Quantum Elec.*, 1985, **QE-21**, 1600.
- <sup>37</sup> Halbout, J.-M.; Blit, S.; Donaldson, W. and Tang, C. L., *IEEE J. Quantum Elec.*, 1979, **QE-15**, 1176.
- <sup>38</sup> Pluta, T. and Sadlej, A. J., *J. Chem. Phys.*, 2001, **114**, 136.
- <sup>39</sup> Birkedal, H.; Madsen, D.; Mathiesen, R. H.; Knudsen, K.; Weber, H. P.; Pattison, P. and Schwarzenbach, D., *Acta Crystallogr. Sec. A*, 2004, **60**, 371–381.
- <sup>40</sup> Born, M. and Huang, K., *Dynamical Theory of Crystal Lattices*, Oxford Univ. Press, Oxford, 1954.
- <sup>41</sup> Zicovich-Wilson, C. M.; Torres, F. J.; Pascale, F.; Valenzano, L.; Orlando, R. and Dovesi, R., *J. Comp. Chem.*, 2008, **29**, 2268–2278.
- <sup>42</sup> Hammond, R.; Pencheva, K.; Roberts, K. J.; Mougín, P. and Wilkinson, D., *J. Appl. Cryst.*, 2005, **38**, 1038–1039.

- <sup>43</sup> Janesko, B. G.; Henderson, T. M. and Scuseria, G. E., *Phys. Chem. Chem. Phys.*, 2009, **11**, 443–454.
- <sup>44</sup> Kirtman, B.; Bonness, S.; Ramirez-Solis, A.; Champagne, B.; Matsumoto, H. and Sekino, H., *J. Chem. Phys.*, 2008, **128**, 114108.
- <sup>45</sup> Benková, Z.; Cernusák, I. and Zahradník, P., *Int. J. Quantum Chem.*, 2007, **107**, 21332152.

## Figures

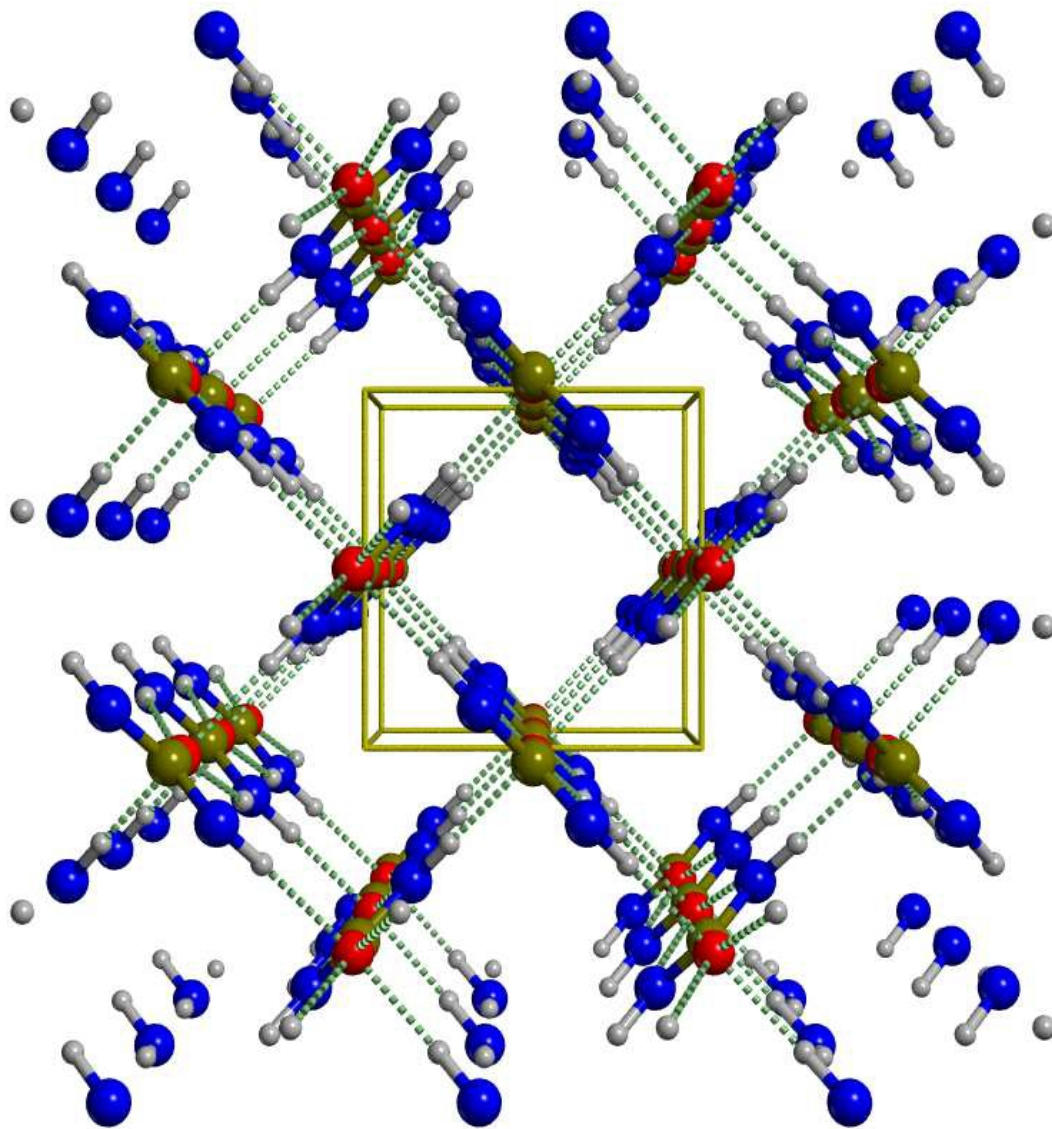


FIG. 1: Unit cell and crystal packing in solid urea as view along the  $c$ -axis



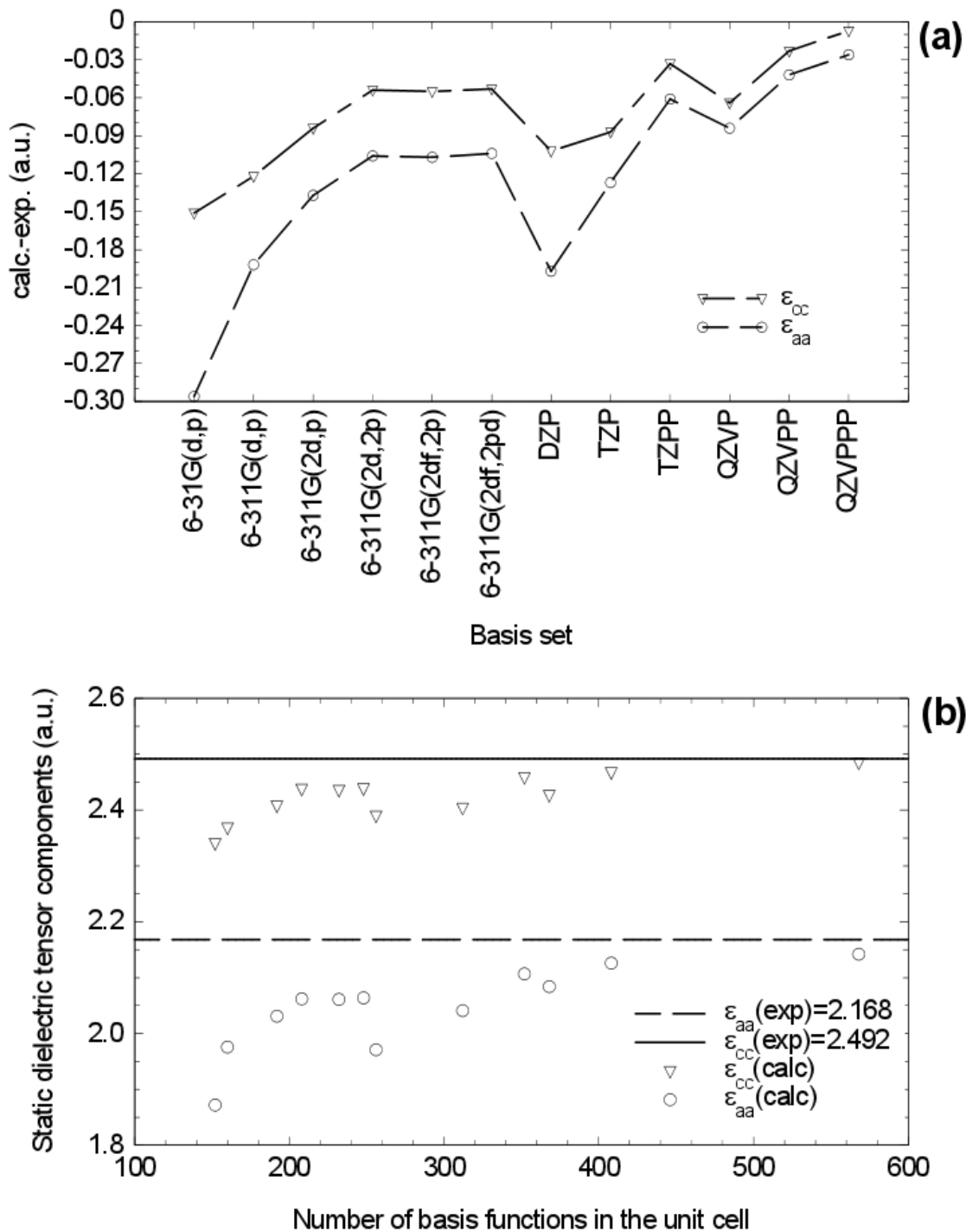


FIG. 2: (a) Deviation from experimental values of the B3LYP dielectric tensor elements  $\epsilon_{aa}$  and  $\epsilon_{cc}$  as a function of the basis set employed. (b) Dependence of the B3LYP static dielectric tensor elements  $\epsilon_{aa}$  and  $\epsilon_{cc}$  on the number of atomic orbitals in the unit cell. Solid and dash lines: experimental values (in a.u.)



TABLE 1: Basis set dependence of the polarizability ( $\alpha_{aa}$  and  $\alpha_{cc}$ ) of free urea molecule and urea bulk (per molecule) at the B3LYP level of theory. Comparison between the results obtained by using the geometry (at fixed planar  $C_{2v}$  conformation) as fully optimized and extracted from the bulk structure. Data in a.u. The ratio between polarizability of the crystal and the molecule as in the bulk is given in parentheses.

| Basis set       | Molecule $C_{2v}$ |               |                |               | Crystal        |                |
|-----------------|-------------------|---------------|----------------|---------------|----------------|----------------|
|                 | Fully optimized   |               | Bulk structure |               | $\alpha_{aa}$  | $\alpha_{cc}$  |
|                 | $\alpha_{aa}$     | $\alpha_{cc}$ | $\alpha_{aa}$  | $\alpha_{cc}$ | $\alpha_{aa}$  | $\alpha_{cc}$  |
| 6-31G(d,p)      | 21.970            | 32.560        | 22.020         | 33.259        | 33.975 (1.543) | 52.215 (1.570) |
| 6-311G(d,p)     | 24.554            | 33.400        | 24.597         | 34.057        | 38.012 (1.545) | 53.337 (1.566) |
| 6-311G(2d,p)    | 26.059            | 34.231        | 26.103         | 34.891        | 40.154 (1.538) | 54.821 (1.571) |
| 6-311G(2d,2p)   | 26.880            | 34.894        | 26.927         | 35.519        | 41.345 (1.535) | 55.996 (1.576) |
| 6-311G(2df,2p)  | 26.958            | 35.020        | 26.942         | 35.541        | 41.318 (1.534) | 55.938 (1.574) |
| 6-311G(2df,2pd) | 26.994            | 35.020        | 27.035         | 35.633        | 41.425 (1.532) | 56.035 (1.573) |
| DZP             | 24.070            | 34.192        | 24.182         | 34.869        | 37.812 (1.564) | 54.135 (1.553) |
| TZP             | 26.920            | 36.047        | 26.943         | 36.797        | 40.557 (1.505) | 54.694 (1.486) |
| TZPP            | 28.718            | 37.129        | 28.737         | 37.801        | 43.127 (1.501) | 56.822 (1.503) |
| QZVP            | 28.554            | 37.183        | 28.565         | 38.030        | 42.230 (1.478) | 55.588 (1.462) |
| QZVPP           | 30.027            | 38.067        | 30.020         | 38.816        | 43.840 (1.460) | 57.194 (1.473) |
| QZVPPP          | 31.033            | 38.931        | 31.031         | 39.679        | 44.481 (1.433) | 57.829 (1.457) |

TABLE 2: Comparison between HF and DFT methods for the polarizability ( $\alpha_{aa}$  and  $\alpha_{cc}$ ) of free urea molecule and urea bulk (per molecule) computed with the TZPP basis set. Comparison between the results obtained by using the geometry (at fixed planar  $C_{2v}$  conformation) as fully optimized and extracted from the bulk structure. Data in a.u.. The ratio between polarizability of the crystal and the molecule as in the bulk is given in parentheses.

| Method | Molecule $C_{2v}$             |                               |                              |                              | Crystal        |                |
|--------|-------------------------------|-------------------------------|------------------------------|------------------------------|----------------|----------------|
|        | Fully optimized $\alpha_{aa}$ | Fully optimized $\alpha_{cc}$ | Bulk structure $\alpha_{aa}$ | Bulk structure $\alpha_{cc}$ | $\alpha_{aa}$  | $\alpha_{cc}$  |
| SVWN   | 30.088                        | 38.857                        | 30.460                       | 40.265                       | 49.122 (1.613) | 64.472 (1.601) |
| PBE    | 30.251                        | 39.138                        | 30.378                       | 40.060                       | 47.329 (1.558) | 62.777 (1.567) |
| B3LYP  | 28.718                        | 37.129                        | 28.737                       | 37.801                       | 43.127 (1.501) | 56.822 (1.503) |
| PBE0   | 28.269                        | 36.519                        | 28.326                       | 37.224                       | 42.408 (1.497) | 55.766 (1.498) |
| HF     | 25.211                        | 32.524                        | 25.150                       | 32.762                       | 34.814 (1.384) | 44.604 (1.361) |

TABLE 3: Basis set dependence of the optical dielectric tensor elements ( $\epsilon_{aa}$  and  $\epsilon_{cc}$ ), refractive indices ( $n_{aa}$  and  $n_{cc}$ ) and birefringence parameters ( $\delta^{(1)}$  and  $\Delta n$ ) for crystalline urea at the B3LYP level of theory. Data in a.u.

| Basis set                   | $\epsilon_{aa}$ | $\epsilon_{cc}$ | $n_{aa}$ | $n_{cc}$ | $\delta^{(1)}$ | $\Delta n$ |
|-----------------------------|-----------------|-----------------|----------|----------|----------------|------------|
| 6-31G(d,p)                  | 1.872           | 2.341           | 1.368    | 1.530    | 0.118          | 0.162      |
| 6-311G(d,p)                 | 1.976           | 2.369           | 1.406    | 1.539    | 0.095          | 0.134      |
| 6-311G(2d,p)                | 2.031           | 2.408           | 1.425    | 1.552    | 0.089          | 0.127      |
| 6-311G(2d,2p)               | 2.062           | 2.438           | 1.436    | 1.561    | 0.087          | 0.125      |
| 6-311G(2df,2p)              | 2.061           | 2.436           | 1.436    | 1.561    | 0.087          | 0.125      |
| 6-311G(2df,2pd)             | 2.064           | 2.439           | 1.437    | 1.562    | 0.087          | 0.125      |
| DZP                         | 1.971           | 2.390           | 1.404    | 1.546    | 0.101          | 0.142      |
| TZP                         | 2.041           | 2.423           | 1.429    | 1.551    | 0.085          | 0.122      |
| TZPP                        | 2.107           | 2.459           | 1.452    | 1.568    | 0.080          | 0.116      |
| QZVP                        | 2.084           | 2.427           | 1.444    | 1.558    | 0.079          | 0.114      |
| QZVPP                       | 2.126           | 2.468           | 1.458    | 1.571    | 0.078          | 0.113      |
| QZVPPP                      | 2.142           | 2.485           | 1.464    | 1.576    | 0.077          | 0.113      |
| Exp. (static) <sup>37</sup> | 2.168           | 2.492           | 1.472    | 1.579    | 0.072          | 0.106      |

TABLE 4: Comparison between HF and DFT methods for the optical dielectric tensor elements ( $\epsilon_{aa}$  and  $\epsilon_{cc}$ ), refractive indices ( $n_{aa}$  and  $n_{cc}$ ), birefringence parameters ( $\delta^{(1)}$  and  $\Delta n$ ) and band gap ( $E_g$ , in eV) of crystalline urea computed with a TZPP basis set. Data in a.u.

| Method                                   | $\epsilon_{aa}$ | $\epsilon_{cc}$ | $n_{aa}$ | $n_{cc}$ | $\delta^{(1)}$ | $\Delta n$ | $E_g$                |
|--|-----------------|-----------------|----------|----------|----------------|------------|----------------------|
| <i>Present work</i>                      |                 |                 |          |          |                |            |                      |
| SVWN                                     | 2.261           | 2.655           | 1.504    | 1.630    | 0.084          | 0.126      | 4.80                 |
| PBE                                      | 2.215           | 2.612           | 1.488    | 1.616    | 0.086          | 0.128      | 5.17                 |
| B3LYP                                    | 2.107           | 2.459           | 1.452    | 1.568    | 0.080          | 0.116      | 6.92                 |
| PBE0                                     | 2.089           | 2.432           | 1.445    | 1.559    | 0.079          | 0.114      | 7.43                 |
| HF                                       | 1.894           | 2.145           | 1.376    | 1.465    | 0.064          | 0.088      | 14.08                |
| <i>Other theoretical predicted data</i>  |                 |                 |          |          |                |            |                      |
| LDA (1064 nm) <sup>a</sup>               | 2.261           | 2.640           | 1.504    | 1.625    | 0.080          | 0.121      | 4.27                 |
| LDA no local-field <sup>b</sup>          | 2.270           | 2.473           | 1.507    | 1.573    | 0.044          | 0.066      | 5.50                 |
| LDA local-field <sup>b</sup>             | 2.029           | 2.143           | 1.424    | 1.464    | 0.028          | 0.039      | 5.50                 |
| AM1/ $F^{\alpha,CCSD}$ <sup>c</sup>      | 1.940           | 2.140           | 1.393    | 1.463    | 0.050          | 0.070      |                      |
| AM1/ $F^{\alpha,CAM-B3LYP}$ <sup>c</sup> | 1.890           | 2.070           | 1.375    | 1.439    | 0.047          | 0.064      |                      |
| RLFT4 MP2 no local-field <sup>d</sup>    | 2.153           | 2.729           | 1.467    | 1.652    | 0.126          | 0.185      |                      |
| RLFT4 MP2 local-field <sup>d</sup>       | 2.180           | 2.693           | 1.476    | 1.641    | 0.111          | 0.165      |                      |
| X-ray/RLFT4 <sup>e</sup>                 | 2.220           | 2.723           | 1.490    | 1.650    | 0.107          | 0.160      |                      |
| Exp. (static) <sup>f</sup>               | 2.168           | 2.492           | 1.472    | 1.579    | 0.072          | 0.106      | 5.7-6.2 <sup>g</sup> |

<sup>a,b</sup> Band structure calculation at LDA level within a pseudopotentials/planewaves.

theoretical frame from ref. 15 and 11, respectively.

<sup>c</sup> Supermolecule approach and multiplicative scheme. See ref. 18.

<sup>d</sup> Rigorous Local-Field Theory (RLFT) approach. Ref. 12.

<sup>e</sup> X-ray fitted wavefunction combine with a RLFT4 scheme. Ref. 17.

<sup>f</sup> From data extrapolated to the static limit<sup>37</sup>.

<sup>g</sup> For band gap see references in ref. 11.

TABLE 5: Basis set dependence at the B3LYP level and comparison between HF and DFT methods (TZPP basis set) for the static first-hyperpolarizability ( $\beta_{abc}$ ) of urea molecule (at fixed planar  $C_{2v}$  conformation) as fully optimized and extracted from the bulk structure, and crystalline urea (per molecule). For the crystal, the second-susceptibility ( $\chi_{abc}^{(2)}$ ) and the second-harmonic nonlinear coefficient ( $d_{14}$ ) are also reported. Data in a.u. if not otherwise specified. The ratio between first-hyperpolarizability of the crystal and the molecule as in the bulk is given in parentheses

|              | Molecule $C_{2v}$ |                | Crystal          |                    |                 |
|--------------|-------------------|----------------|------------------|--------------------|-----------------|
|              | Fully optimized   | Bulk structure | $\beta_{abc}$    | $\chi_{abc}^{(2)}$ | $d_{14}$ (pm/V) |
| <i>B3LYP</i> |                   |                |                  |                    |                 |
| TZPP         | -18.140           | -15.385        | -72.772 (4.730)  | -0.934             | -0.908          |
| QZVPP        | -21.616           | -18.803        | -73.277 (3.897)  | -0.941             | -0.915          |
| QZVPPP       | -21.193           | -18.580        | -70.770 (3.809)  | -0.909             | -0.883          |
| <i>TZPP</i>  |                   |                |                  |                    |                 |
| HF           | -22.065           | -22.122        | -52.565 (2.376)  | -0.675             | -0.656          |
| SVWN         | -10.756           | -5.082         | -91.721 (18.047) | -1.177             | -1.145          |
| PBE          | -9.745            | -4.072         | -82.363 (20.227) | -1.057             | -1.028          |
| PBE0         | -19.266           | -17.199        | -68.879 (4.005)  | -0.884             | -0.860          |
| B3LYP        | -18.140           | -15.385        | -72.772 (4.730)  | -0.934             | -0.908          |